PERGAMON

International Journal of Solids and Structures 40 (2003) 1745–1764

INTERNATIONAL JOURNAL OF SOLIDS and STRUCTURES

www.elsevier.com/locate/ijsolstr

# Three-dimensional modelling of elastic bonding in composite laminates using layerwise differential quadrature

K.M. Liew [a,*], Jordan Z. Zhang [a], T.Y. Ng [a,b], S.A. Meguid [c]

[a] *Nanyang Centre for Supercomputing and Visualisation, School of Mechanical and Production Engineering, Nanyang Technological University, Nanyang Avenue, Singapore 639798, Singapore*

[b] *Institute of High Performance Computing, 89C Science Park Drive, #02-11/12, The Rutherford, Singapore Science Park 1, Singapore 118261, Singapore*

[c] *Engineering Mechanics and Design Laboratory, University of Toronto, 5 King's College Road, Toronto, Ont., Canada M5S 3G8*

Received 30 October 2001; received in revised form 11 November 2002

**Abstract**

In an effort to overcome the limitations of existing rigid bonding analysis of composite laminates, the current three-dimensional elastostatic model is proposed. In this model, the three-dimensional interlaminar elastic stress field is determined using the technique of layerwise differential quadrature. The new formulations allowed us to determine the influence of a natural bonding layer upon the field variables in the laminated structure. The interfacial characteristics of continuity and discontinuity satisfy the kinematic continuity conditions through the elastic-bonding layer. A number of case studies are examined, comparisons with rigid bonding and finite element analyses are provided, and the influence of the pertinent parameters on the interlaminar stress field is evaluated and discussed.


*Keywords:* Composite laminates; Differential quadrature method; Three-dimensional elasticity theory; Elastic bonding; Rigid bonding; Weak bonding; Finite element analysis

## 1. Introduction

### 1.1. Background

Materials of laminated composite constitution have been utilized in a broad range of engineering applications, such as space and underwater exploration, aircraft structures, electronic and medical components, high-end sporting equipment, just to name a few. In view of the anisotropic nature and complexities of composite multi-layered bonded laminates, various modelling techniques had been proposed. To predict the mechanical performance of laminated plates, for example, Ambartsumyan (1970), Reddy (1984a), Whitney (1987), and Whitney and Leissa (1969), used the classical plate theory to approximate the overall

* Corresponding author. Tel.: +65-6790-4076; fax: +65-6790-6763.
*E-mail address:* mkmliew@ntu.edu.sg (K.M. Liew).

0020-7683/02/$ - see front matter © 2002 Elsevier Science Ltd. All rights reserved.
doi:10.1016/S0020-7683(02)00666-2

response of the laminates. This is because the theory treats the plates as being infinitely rigid in the transverse direction. The first and third-order theories (Stavsky, 1965; Yang et al., 1966; Whitney and Pagano, 1970; Reddy, 1984b,c), to a certain extent, remedy these defects. However, the equivalent single layer theory, directly evolved from conventional plate theory, remains unable to provide an accurate assessment of the distribution of the stress components at the ply level. Noting these restrictions in traditional plate and shell theories, the layerwise theory of Reddy (1987, 1989) was developed. Reddy assumed separate displacement fields for each lamina, and compared with the equivalent single layer theories, providing a possibility for accommodating the kinematical characteristics of the laminate. Distinct from the numerous plate theories, Srinivas and Rao (1970) adopted three-dimensional elasticity theory to develop an analytical model for laminated structures. They provided results for simply supported square sandwich laminates. For other combinations of edge-support conditions, Liew et al. (2002) presented a set of three-dimensional elasticity solutions for cross-ply laminates using the differential quadrature (DQ)-layerwise modeling technique.

In the conventional analysis of laminated composites mentioned above, the composite interfaces are always assumed to be rigidly bonded, i.e., the displacements of the composite interfaces are single valued. The influence of the relatively low shear modulus of the matrix material is most prevalent at the ply interface. This fact, coupled with the possible defective bonding of laminates, may lead to an elastic or weak interlayer connection. Indeed, it has been recognized, see Lu and Liu (1992), that the low shear modulus of the polymer matrix materials has significant effects on the transverse shear deformation. Consequently, the interfacial conditions can strongly affect the service characteristics of laminates. In order to provide a proper assessment of the performance of composite laminates, it is of vital importance to account for the bonding condition accurately. This can be achieved by combining the transverse shear effects with the continuity requirements for both displacements and interlaminar stresses of the composite interface.

The study of non-rigidly bonded interfaces in composite structures was pioneered by Newmark et al. (1951) and later by Goodman (1967), where based on the Euler–Bernoulli beam theory, a laminated beam theory with linear shear slip in the layer interface was developed. Toledano and Murakami (1988) used a laminate theory, accounting for both transverse shear effect and interlaminar shear stress continuity, to study non-rigid bonding effects. Elastic studies of sandwich beams with non-rigid bonding were also presented by Rao and Ghosh (1980) and Fazio et al. (1982).

There are basically three model types of weak bonding between layers. They are shear modelling with slip between layers; normal separation modelling with an opening between layers; and general weak bonding that combines both of the preceding models. The concept of weakly bonded layers has been introduced by permitting a certain displacement jump, see Lu and Liu (1992) and Liu et al. (1994), at an interface. These authors related the interfacial jump to the interlaminar stress, through appropriate constitutive relations, which establish an equivalent stiffness along the jump direction.

In this paper, the authors overcame some of the limitations of existing rigid and non-rigid models by adopting an innovative technique, which considers the elasticity of the bonding layer using three dimensional elasticity and the DQ method. In the following section, we provide a brief summary of the DQ method.

### *1.2. Differential quadrature method*

In spite of its flexibility and readiness to deal with most engineering problems, in the current application the finite element method suffers from the following drawbacks. First, the size anomaly between the laminae and the bonding layers presents severe difficulties in discretisation. Either a very extensive use of elements is required or a highly distorted mesh is tolerated, thus affecting the accuracy of the results. Second, in view of the three-dimensional nature of the considered problem, it is very difficult to obtain an assessment of the resulting error level. Third, it is a numerical method requiring the appropriate software and experience to apply it properly.

Therefore, there is much incentive to develop more accurate analytical modelling tools for treating composite laminates. The DQ method is a prospective numerical alternative originated by Bellman (1973) to solve linear and nonlinear differential equations. The basic idea of the DQ method is that the partial derivative of a function with respect to a variable at a given discrete point can be approximated as a weighted linear sum of the function values at all discrete points in the domain of that variable, i.e.,

$$f'(x_i) \cong \sum_{j=1}^{N_g} A_{ij} f(x_j), \quad i = 1, 2, \ldots, N_g \tag{1}$$

where $f(x)$ is the function that represents the real physical field, $N_g$ is the number of spacing grid points, and $A_{ij}$ the weighting coefficients to be determined. The DQ method is briefly outlined here and the readers are advised to see Shu (1991) for further details. Let us select the trial function $V_\Theta(x)$ to be Lagrange's interpolation polynomials, viz,

$$V_\Theta(x) = \frac{L_{N_g}(x)}{(x - x_\Theta) L^{[1]}_{N_g}(x_\Theta)}, \quad \Theta = 1, 2, \ldots, N_g \tag{2}$$

where

$$L_{N_g}(x) = \prod_{\alpha=1}^{N_g} (x - x_\alpha) \tag{3}$$

$L^{[1]}_{N_g}(x_\Theta)$ is the first derivatives of $L_{N_g}(x)$ with respect to $x$

$$L^{[1]}_{N_g}(x_\Theta) = \prod_{\substack{\alpha=1 \\ \Theta \neq \alpha}}^{N_g} (x_\Theta - x_\alpha) \tag{4}$$

Substituting Eq. (2) into Eq. (1), the weighting coefficients of the first order derivatives are

$$\begin{cases} A^{\{1\}}_{i\alpha} = \frac{L^{[1]}_{N_g}(x_i)}{(x_i - x_\alpha) L^{[1]}_{N_g}(x_\alpha)}, & i \neq \alpha \\ A^{\{1\}}_{ii} = \frac{L^{[2]}_{N_g}(x_i)}{2 L^{[1]}_{N_g}(x_i)}, & i = \alpha \end{cases} \tag{5}$$

Similarly, we may obtain the weighting coefficients for higher-order derivative through this scheme. The coordinate variable $x$ with the subscript $i$ refers to the spatial position of the grid point, and the usual spacing patterns of these grid points in the DQ method are

$$\text{(I) Equal spacing :} \qquad x_i = \frac{i-1}{N_g - 1}, \quad i = 1, 2, \ldots, N_g \tag{6}$$

and

$$\text{(II) Cosine spacing :} \qquad x_i = \frac{1 - \cos \frac{i-1}{N_g - 1} \pi}{2}, \quad i = 1, 2, \ldots, N_g \tag{7}$$

The latter spacing pattern is employed in this paper because of its stable convergence characteristics in plate analysis (Liew et al., 1999, 2001).

The advantages of the DQ method lie in the simplicity of the devised algorithms and the use of gross grid point distributions, leading to efficient computation and flexible discretization. It also has the added advantage of providing highly accurate results, because it implements higher-order interpolation (shape) functions with ease.

Since its introduction, the DQ method has been applied to various engineering mechanics problems, such as bending, vibration and buckling of beams, columns and plates, including thin, thick and laminated composite plates. The successful implementation of this method has been reported in literature; see the works of Bert et al. (1988), Jang et al. (1989), Farsa et al. (1993) and Han and Liew (1997). These works, amongst others, culminated in a comprehensive review of the development and application of DQ method in computational mechanics presented by Bert and Malik (1996).

## 2. Interface modelling in elastic bonding

### 2.1. Physical model of elastic bonding

Consider a rectangular $L$-layer laminate, $L$ being the total number of layers, and $h_i$ the thickness of the $i$th lamina, as depicted in Fig. 1. Any two adjacent laminae are bonded together, particularly in the intermediate region of the composite, by a natural (isotropic or anisotropic) layer of thickness $h$. $h$ is assumed to be very thin in comparison with the thickness of the adjacent laminae. For example, $h/h^k \sim 0.001$, with $h^k$ being the thickness of the $k$th layer of the laminate. Since each layer consists of fibres, which are randomly distributed in the matrix, the considered system can be regarded as homogenous and isotropic.

In the current model, the natural layer is assumed to be rigidly bonded to the neighbouring laminae. Consequently, the continuity conditions of displacements are satisfied, and the continuity conditions of the transverse stresses are enforced along the interfaces between the bonding layer and each of the neighbouring laminae. The rigid bonding model, on the other hand, does not cater for any deformable behaviour along the interface of two bordering laminae. It is also worth noting that the weak bonding model accounts for the relative movement through a series of independent three dimensional springs linking two material points, initially on opposite sides of the interface, via constitutive relations of displacement jumps and the corresponding stresses. The shortcomings of the latter are twofold. First, discrete springs are incapable of capturing the bonding interaction between layers. Second, the stiffnesses of the springs in three spatial directions of one material point are difficult to determine accurately as the stiffnesses are mutually related.

### 2.2. Theoretical model of elastic bonding

To establish a precise theoretical basis for elastic bonding suitable for the diverse situations encountered in engineering applications, the authors propose to integrate three-dimensional elasticity theory within the framework of layerwise theory.

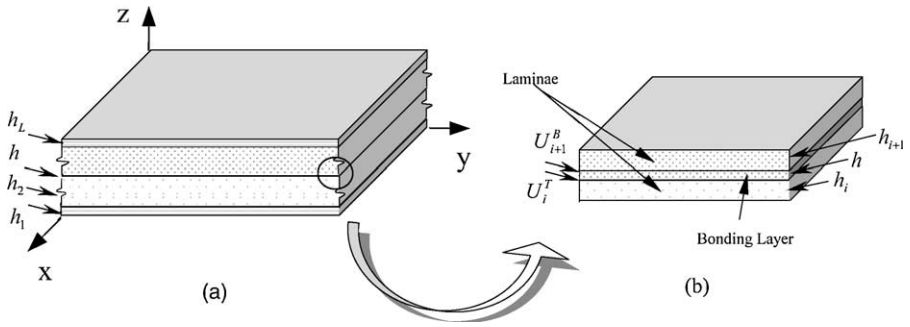


Fig. 1. The laminated plate structure with the bonding layers.

Supposing that the displacements in the $x$, $y$ and $z$ directions $U_i$, $V_i$ and $W_i$, of the $i$th layer are given by

$$U_i = u_i(x,y,z), \quad V_i = v_i(x,y,z), \quad W_i = w_i(x,y,z), \quad i = 1,2,3,\ldots L \tag{8}$$

then the strain–displacement relations can be written as

$$\begin{aligned} &\varepsilon_x = \frac{\partial u}{\partial x}, \quad \varepsilon_y = \frac{\partial v}{\partial y}, \quad \varepsilon_z = \frac{\partial w}{\partial z} \\ &\gamma_{xy} = \frac{\partial u}{\partial y} + \frac{\partial v}{\partial x}, \quad \gamma_{yz} = \frac{\partial v}{\partial z} + \frac{\partial w}{\partial y}, \quad \gamma_{zx} = \frac{\partial w}{\partial x} + \frac{\partial u}{\partial z} \end{aligned} \tag{9}$$

where $\varepsilon_x$, $\varepsilon_y$ and $\varepsilon_z$ are the normal strains, $u$, $v$, $w$ are displacements in $x$, $y$, $z$ directions, and $\gamma_{xy}$, $\gamma_{yz}$, and $\gamma_{zx}$ are the shear strains in the $x$–$y$, $y$–$z$ and $z$–$x$ planes, respectively. Substituting Eq. (8) into Eq. (9), we obtain the strain field for the $i$th layer

$$\begin{aligned} &\varepsilon_x^{(i)} = \frac{\partial U_i}{\partial x}, \quad \varepsilon_y^{(i)} = \frac{\partial V_i}{\partial y}, \quad \varepsilon_z^{(i)} = \frac{\partial W_i}{\partial z} \\ &\gamma_{xy}^{(i)} = \frac{\partial U_i}{\partial y} + \frac{\partial V_i}{\partial x}, \quad \gamma_{yz}^{(i)} = \frac{\partial V_i}{\partial z} + \frac{\partial W_i}{\partial y}, \quad \gamma_{zx}^{(i)} = \frac{\partial W_i}{\partial x} + \frac{\partial U_i}{\partial z} \end{aligned} \tag{10}$$

The constitutive relations are written as

$$\left\{\sigma_x, \sigma_y, \sigma_z, \tau_{yz}, \tau_{zx}, \tau_{xy}\right\}^{\mathrm{T}} = [C_{ij}] \cdot \left\{\varepsilon_x, \varepsilon_y, \varepsilon_z, \gamma_{yz}, \gamma_{zx}, \gamma_{xy}\right\}^{\mathrm{T}} \tag{11}$$

where $\sigma_x$, $\sigma_y$, $\sigma_z$ are normal stresses, $\tau_{yz}$, $\tau_{zx}$, $\tau_{xy}$ are shear stresses, and $C_{ij}$ $(i,j = 1,2,\ldots,6)$ is the stiffness matrix. The equations of equilibrium for each laminae and bonding layer are

$$\frac{\partial \sigma_x}{\partial x} + \frac{\partial \tau_{xy}}{\partial y} + \frac{\partial \tau_{xz}}{\partial z} = 0, \quad \frac{\partial \sigma_y}{\partial y} + \frac{\partial \tau_{xy}}{\partial x} + \frac{\partial \tau_{yz}}{\partial z} = 0, \quad \frac{\partial \sigma_z}{\partial z} + \frac{\partial \tau_{xz}}{\partial x} + \frac{\partial \tau_{yz}}{\partial y} = 0 \tag{12}$$

In this work, it is proposed that the variations of the thickness components of the transverse strains are proportional to the displacement jump between the surfaces of the bonding layer. This assumption is reasonable and can be justified by the fact that the bonding layer is typically thin.

At the interface between the $i$th lamina and a bonding layer,

$$\varepsilon_z^{(i)} = -\frac{W_i^u - W_{i+1}^d}{h}, \quad \gamma_{yz}^{(i)} = \frac{V_i^u - V_{i+1}^d}{h} + \frac{\partial W_i}{\partial y}, \quad \gamma_{zx}^{(i)} = \frac{\partial W_i}{\partial x} + \frac{U_i^u - U_{i+1}^d}{h} \tag{13.1}$$

and at the interface between a bonding layer and $i+1$th lamina

$$\varepsilon_z^{(i+1)} = -\frac{W_i^u - W_{i+1}^d}{h}, \quad \gamma_{yz}^{(i+1)} = -\frac{V_i^u - V_{i+1}^d}{h} + \frac{\partial W_i}{\partial y}, \quad \gamma_{zx}^{(i+1)} = \frac{\partial W_i}{\partial x} - \frac{U_i^u - U_{i+1}^d}{h} \tag{13.2}$$

where the superscripts $u$ and $d$ refer to the upper and lower surfaces of the bonding layer, respectively.

From Eq. (13), it should be noted that only the transverse components of the strains are linearly simplified, while the in-plane components remain unchanged. This is crucial for the present model, which accounts for the effects of in-plane deformation in the bonding layers. Distinct from the discrete spring model of weak bonding, the present model is treated as a continuum.

The simply supported edge conditions can be defined as

$$\begin{aligned} &w = \sigma_x = \tau_{xy} = 0, \quad \text{at the edges of } x = \text{constant} \\ &w = \sigma_y = \tau_{xy} = 0, \quad \text{at the edges of } y = \text{constant} \end{aligned} \tag{14.1}$$

while the clamped edge conditions can be defined as

$$u = v = w = 0, \quad \text{at the edges of } x, y = \text{constant} \tag{14.2}$$

and the surface conditions as being

$$\begin{aligned} &\sigma_z = \tau_{xz} = \tau_{yz} = 0, \quad \text{at bottom of laminate} \\ &\sigma_z = -q, \quad \tau_{xz} = \tau_{yz} = 0, \quad \text{at top of laminate} \end{aligned} \tag{15}$$

where $q$ is the surface loading.

Obviously, the interfacial characteristics of rigid bonding such as continuity/discontinuity of displacements, and strains and stresses no longer hold, and the corresponding constraints are transferred through the material bonding layer, Fig. 1(b). At the interface between the lower lamina and the bonding layer, the constraints of continuity of the elastic bonding are

$$\begin{Bmatrix} \sigma_z^{(i)} \\ \tau_{zx}^{(i)} \\ \tau_{zy}^{(i)} \end{Bmatrix}_{\text{top}} = \begin{Bmatrix} \sigma_z^{(\text{BL})} \\ \tau_{zx}^{(\text{BL})} \\ \tau_{zy}^{(\text{BL})} \end{Bmatrix}_{\text{bottom}}, \quad i = 1, 2, \ldots, L-1 \tag{16}$$

and at the interface between the bonding layer and the upper lamina are

$$\begin{Bmatrix} \sigma_z^{(\text{BL})} \\ \tau_{zx}^{(\text{BL})} \\ \tau_{zy}^{(\text{BL})} \end{Bmatrix}_{\text{top}} = \begin{Bmatrix} \sigma_z^{(i+1)} \\ \tau_{zx}^{(i+1)} \\ \tau_{zy}^{(i+1)} \end{Bmatrix}_{\text{bottom}}, \quad i = 2, \ldots, L-1, L \tag{17}$$

where the superscripts of the stress notations, $i$ or $i+1$, indicate the lamina position, and BL refers to the bonding layer. According to DQ methodology, all governing equations can be expressed in terms of the derivatives of displacements. Thus, the results obtained from this model are accurate three-dimensional numerical solutions. Substituting Eq. (9) into Eq. (11), and assuming orthotropy of the laminae, we can obtain

$$\begin{aligned} &\sigma_x = C_{11}\frac{\partial u}{\partial x} + C_{12}\frac{\partial v}{\partial y} + C_{13}\frac{\partial w}{\partial z}, \quad \sigma_y = C_{21}\frac{\partial u}{\partial x} + C_{22}\frac{\partial v}{\partial y} + C_{23}\frac{\partial w}{\partial z}, \quad \sigma_z = C_{31}\frac{\partial u}{\partial x} + C_{32}\frac{\partial v}{\partial y} + C_{33}\frac{\partial w}{\partial z} \\ &\tau_{yz} = C_{44}\left(\frac{\partial v}{\partial z} + \frac{\partial w}{\partial y}\right), \quad \tau_{zx} = C_{55}\left(\frac{\partial w}{\partial x} + \frac{\partial u}{\partial z}\right), \quad \tau_{xy} = C_{66}\left(\frac{\partial u}{\partial y} + \frac{\partial v}{\partial x}\right) \end{aligned} \tag{18}$$

For simplicity, the following variables are normalised as

$$\begin{aligned} &X = \frac{x}{a}, \quad Y = \frac{y}{b}, \quad Z_i = \frac{z}{h_i} \\ &\overline{U} = \frac{u}{a}, \quad \overline{V} = \frac{v}{b}, \quad \overline{W} = \frac{w}{H} \end{aligned} \tag{19}$$

where $Z_i$ is the thickness coordinate of the $i$th layer, $a$ and $b$ are the length and width of the laminate, respectively. Let us now define

$$\begin{aligned} &H = \sum h_i + (L-1)\cdot h \\ &\frac{b}{a} = B_{\text{p}}, \quad \frac{h_i}{a} = D_i, \quad \frac{H}{h_i} = H_i \end{aligned} \tag{20}$$

The normalised equilibrium equations for the $i$th lamina ($i = 1, 2, \ldots, L$) can then be expressed as

$$\begin{aligned}
&B_p^2 C_{11}\frac{\partial^2 \overline{U}}{\partial X^2} + C_{66}\frac{\partial^2 \overline{U}}{\partial Y^2} + \left(\frac{B_p}{D_i}\right)^2 C_{55}\frac{\partial^2 \overline{U}}{\partial Z_i^2} + B_p^2(C_{12}+C_{66})\frac{\partial^2 \overline{V}}{\partial X \partial Y} + B_p^2 H_i(C_{13}+C_{55})\frac{\partial^2 \overline{W}}{\partial X \partial Z_i} = 0\\
&\frac{1}{B_p^2}(C_{21}+C_{66})\frac{\partial^2 \overline{U}}{\partial X \partial Y} + C_{66}\frac{\partial^2 \overline{V}}{\partial X^2} + \frac{1}{B_p^2}C_{22}\frac{\partial^2 \overline{V}}{\partial Y^2} + \frac{1}{D_i^2}C_{44}\frac{\partial^2 \overline{V}}{\partial Z_i^2} + \frac{H_i}{B_p^2}(C_{23}+C_{44})\frac{\partial^2 \overline{W}}{\partial Y \partial Z_i} = 0\\
&\frac{1}{D_i^2}(C_{31}+C_{55})\frac{\partial^2 \overline{U}}{\partial X \partial Z_i} + \frac{1}{D_i^2}(C_{32}+C_{44})\frac{\partial^2 \overline{V}}{\partial Y \partial Z_i} + H_i C_{55}\frac{\partial^2 \overline{W}}{\partial X^2} + \frac{H_i}{B_p^2}C_{44}\frac{\partial^2 \overline{W}}{\partial Y^2} + \frac{H_i}{D_i^2}C_{33}\frac{\partial^2 \overline{W}}{\partial Z_i^2} = 0
\end{aligned} \tag{21}$$

The support conditions of Eq. (14) can be normalised as follows: for the simply supported edge conditions

$$\begin{aligned}
&\overline{W} = 0, \quad C_{11}\frac{\partial \overline{U}}{\partial X} + C_{12}\frac{\partial \overline{V}}{\partial Y} + C_{13}\frac{\partial \overline{W}}{\partial Z_i} = 0, \quad C_{66}\left(\frac{1}{B_p}\frac{\partial \overline{U}}{\partial Y} + B_p\frac{\partial \overline{V}}{\partial X}\right) = 0, \quad \text{at the edges of constant } x\\
&\overline{W} = 0, \quad C_{21}\frac{\partial \overline{U}}{\partial X} + C_{22}\frac{\partial \overline{V}}{\partial Y} + C_{23}\frac{\partial \overline{W}}{\partial Z_i} = 0, \quad C_{66}\left(\frac{1}{B_p}\frac{\partial \overline{U}}{\partial Y} + B_p\frac{\partial \overline{V}}{\partial X}\right) = 0, \quad \text{at the edges of constant } y
\end{aligned} \tag{22.1}$$

and for the clamped edge conditions

$$\overline{U} = \overline{V} = \overline{W} = 0, \quad \text{at the edges of } x, y = \text{constant} \tag{22.2}$$

In view of DQ methodology (Eq. (1)), the equilibrium equations at the interior domain, boundary conditions, and interface continuity conditions can be formulated in terms of displacement variables and the corresponding weighting coefficients in a discretized DQ format.

The normalised DQ equilibrium equations at an interior grid point $(X_k, Y_m, Z_r)$ can be expressed as

$$\begin{aligned}
&B_p^2 C_{11}^{\{i\}}\sum_{j=1}^{K} A_{Xkj}^{[2]}\overline{U}^{(i)}(X_j, Y_m, Z_r) + C_{66}^{\{i\}}\sum_{g=1}^{M} A_{Ymg}^{[2]}\overline{U}^{(i)}(X_k, Y_g, Z_r) + \left(\frac{B_p}{D_i}\right)^2 C_{55}^{\{i\}}\sum_{f=1}^{R_i} A_{Zrf}^{[2]}\overline{U}^{(i)}(X_k, Y_m, Z_f)\\
&\quad + B_p^2\left(C_{12}^{\{i\}} + C_{66}^{\{i\}}\right)\sum_{j=1}^{K} A_{Xkj}^{[1]}\cdot\left[\sum_{g=1}^{M} A_{Ymg}^{[1]}\overline{V}^{(i)}(X_j, Y_g, Z_r)\right]\\
&\quad + B_p^2 H_i\left(C_{13}^{\{i\}} + C_{55}^{\{i\}}\right)\sum_{j=2}^{K-1} A_{Xkj}^{[1]}\cdot\left[\sum_{f=1}^{R_i} A_{Zrf}^{[1]}\overline{W}^{(i)}(X_j, Y_m, Z_f)\right] = 0\\
&\frac{1}{B_p^2}\left(C_{21}^{\{i\}} + C_{66}^{\{i\}}\right)\sum_{g=1}^{M} A_{Ymg}^{[1]}\cdot\left[\sum_{j=1}^{K} A_{Xkj}^{[1]}\overline{U}^{(i)}(X_j, Y_g, Z_r)\right] + C_{66}^{\{i\}}\sum_{j=1}^{K} A_{Xkj}^{[2]}\overline{V}^{(i)}(X_j, Y_m, Z_r)\\
&\quad + \frac{1}{B_p^2}C_{22}^{\{i\}}\sum_{g=1}^{M} A_{Ymg}^{[2]}\overline{V}^{(i)}(X_k, Y_g, Z_r) + \frac{1}{D_i^2}C_{44}^{\{i\}}\sum_{f=1}^{R_i} A_{Zrf}^{[2]}\overline{V}^{(i)}(X_k, Y_m, Z_f)\\
&\quad + \frac{H_i}{B_p^2}\left(C_{23}^{\{i\}} + C_{44}^{\{i\}}\right)\sum_{g=2}^{M-1} A_{Ymg}^{[1]}\cdot\left[\sum_{f=1}^{R_i} A_{Zrf}^{[1]}\overline{W}^{(i)}(X_k, Y_g, Z_f)\right] = 0\\
&\frac{1}{D_i^2}\left(C_{31}^{\{i\}} + C_{55}^{\{i\}}\right)\sum_{j=1}^{K} A_{Xkj}^{[1]}\cdot\left[\sum_{f=1}^{R_i} A_{Zrf}^{[1]}\overline{U}^{(i)}\left(X_j, Y_m, Z_f\right)\right]\\
&\quad + \frac{1}{D_i^2}\left(C_{32}^{\{i\}} + C_{44}^{\{i\}}\right)\sum_{g=1}^{M} A_{Ymg}^{[1]}\cdot\left[\sum_{f=1}^{R_i} A_{Zrf}^{[1]}\overline{V}^{(i)}\left(X_k, Y_g, Z_f\right)\right] + H_i C_{55}^{\{i\}}\sum_{j=2}^{K-1} A_{Xkj}^{[2]}\overline{W}^{(i)}(X_j, Y_m, Z_r)\\
&\quad + \frac{H_i}{B_p^2}C_{44}^{\{i\}}\sum_{g=2}^{M-1} A_{Ymg}^{[2]}\overline{W}^{(i)}(X_k, Y_g, Z_r) + \frac{H_i}{D_i^2}C_{33}^{\{i\}}\sum_{f=1}^{R_i} A_{Zrf}^{[2]}\overline{W}^{(i)}(X_k, Y_m, Z_f) = 0, \quad i = 1, 2, \ldots, L
\end{aligned} \tag{23}$$

where $(X_k, Y_m, Z_r)$ is an interior grid point. $A$'s are the weighting coefficients, whose superscript indicates the order of derivation. The capital letter in the subscript indicates the coordinate direction of derivation, with the lower letters referring to the grid points. $\overline{U}$, $\overline{V}$ and $\overline{W}$ are displacements whose superscript refers to the layer. $K$, $M$, and $R_i$ represent discrete numbers along the $x$, $y$ and $z$ directions within the $i$th layer. The superscript of the stiffness coefficient $C$ of the laminate material refers to the layer sequential number.

The normalised DQ support conditions for different boundaries are given as

For simply supported edge conditions

$$\overline{W}^{(i)}(X_1 \text{ or } X_K, Y_g, Z_f) = 0, \quad i = 1, 2, \ldots, L; \ g = 1, 2, \ldots, M; \ f = 1, 2, \ldots, R_i$$

$$C_{11}^{\{i\}} \sum_{j=1}^{K} A_{X1j}^{[1]} \overline{U}^{(i)}(X_j, Y_g, Z_f) + C_{12}^{\{i\}} \sum_{m=1}^{M} A_{Ygm}^{[1]} \overline{V}^{(i)}(X_1, Y_m, Z_f) + C_{13}^{\{i\}} H_i \sum_{q=1}^{R_i} A_{Zfq}^{[1]} \overline{W}^{(i)}(X_1, Y_g, Z_q) = 0$$

or

$$C_{11}^{\{i\}} \sum_{j=1}^{K} A_{XKj}^{[1]} \overline{U}^{(i)}(X_j, Y_g, Z_f) + C_{12}^{\{i\}} \sum_{m=1}^{M} A_{Ygm}^{[1]} \overline{V}^{(i)}(X_K, Y_m, Z_f) + C_{13}^{\{i\}} H_i \sum_{q=1}^{R_i} A_{Zfq}^{[1]} \overline{W}^{(i)}(X_K, Y_g, Z_q) = 0$$

$$C_{66}^{\{i\}} \left[ B_{\mathrm{p}} \sum_{j=1}^{K} A_{X1j}^{[1]} \overline{V}^{(i)}(X_j, Y_g, Z_f) + \frac{1}{B_{\mathrm{p}}} \sum_{m=1}^{M} A_{Ygm}^{[1]} \overline{U}^{(i)}(X_1, Y_m, Z_f) \right] = 0$$

or

$$C_{66}^{\{i\}} \left[ B_{\mathrm{p}} \sum_{j=1}^{K} A_{XKj}^{[1]} \overline{V}^{(i)}(X_j, Y_g, Z_f) + \frac{1}{B_{\mathrm{p}}} \sum_{m=1}^{M} A_{Ygm}^{[1]} \overline{U}^{(i)}(X_K, Y_m, Z_f) \right] = 0 \quad \text{at the edges of constant } x$$

$$\overline{W}^{(i)}(X_j, Y_1 \text{ or } Y_M, Z_f) = 0, \quad i = 1, 2, \ldots, L; \ j = 1, 2, \ldots, K; \ f = 1, 2, \ldots, R_i$$

$$C_{21}^{\{i\}} \sum_{k=1}^{K} A_{Xjk}^{[1]} \overline{U}^{(i)}(X_k, Y_1, Z_f) + C_{22}^{\{i\}} \sum_{m=1}^{M} A_{Y1m}^{[1]} \overline{V}^{(i)}(X_j, Y_m, Z_f) + C_{23}^{\{i\}} H_i \sum_{q=1}^{R_i} A_{Zfq}^{[1]} \overline{W}^{(i)}(X_j, Y_1, Z_q) = 0$$

or

$$C_{21}^{\{i\}} \sum_{k=1}^{K} A_{Xjk}^{[1]} \overline{U}^{(i)}(X_k, Y_M, Z_f) + C_{22}^{\{i\}} \sum_{m=1}^{M} A_{YMm}^{[1]} \overline{V}^{(i)}(X_j, Y_m, Z_f) + C_{23}^{\{i\}} H_i \sum_{q=1}^{R_i} A_{Zfq}^{[1]} \overline{W}^{(i)}(X_j, Y_M, Z_q) = 0$$

$$C_{66}^{\{i\}} \left[ B_{\mathrm{p}} \sum_{k=1}^{K} A_{Xjk}^{[1]} \overline{V}^{(i)}(X_k, Y_1, Z_f) + \frac{1}{B_{\mathrm{p}}} \sum_{m=1}^{M} A_{Y1m}^{[1]} \overline{U}^{(i)}(X_j, Y_m, Z_f) \right] = 0 \quad \text{or}$$

$$C_{66}^{\{i\}} \left[ B_{\mathrm{p}} \sum_{k=1}^{K} A_{Xjk}^{[1]} \overline{V}^{(i)}(X_k, Y_M, Z_f) + \frac{1}{B_{\mathrm{p}}} \sum_{m=1}^{M} A_{YMm}^{[1]} \overline{U}^{(i)}(X_j, Y_m, Z_f) \right] = 0 \quad \text{at the edges of constant } y \tag{24.1}$$

and for clamped edge conditions

$$\begin{aligned} &\overline{U}^{(i)}(X_1 \text{ or } X_K, Y_g, Z_f) = \overline{V}^{(i)}(X_1 \text{ or } X_K, Y_g, Z_f) = \overline{W}^{(i)}\big(X_1 \text{ or } X_K, Y_g, Z_f\big) = 0 \\ &\qquad i = 1, 2, \ldots, L; \ g = 1, 2, \ldots, M; \ f = 1, 2, \ldots, R_i, \quad \text{at the edges of constant } x \\ &\overline{U}^{(i)}(X_j, Y_1 \text{ or } Y_M, Z_f) = \overline{V}^{(i)}(X_j, Y_1 \text{ or } Y_M, Z_f) = \overline{W}^{(i)}(X_j, Y_1 \text{ or } Y_M, Z_f) = 0 \\ &\qquad i = 1, 2, \ldots, L; \ j = 1, 2, \ldots, K; \ f = 1, 2, \ldots, R_i, \quad \text{at the edges of constant } y \end{aligned} \tag{24.2}$$

The normalised DQ surface conditions at the interior grid points $(X_k, Y_m, 0)$ and $(X_k, Y_m, H)$ can be expressed as

$$C_{31}^{\{1\}}\sum_{j=1}^{K}A_{Xkj}^{[1]}\overline{U}^{(1)}(X_j,Y_m,0)+C_{32}^{\{1\}}\sum_{g=1}^{M}A_{Ymg}^{[1]}\overline{V}^{(1)}(X_k,Y_g,0)+C_{33}^{\{1\}}H_1\sum_{f=1}^{R_1}A_{Z1f}^{[1]}\overline{W}^{(1)}(X_k,Y_m,Z_f)=0$$

$$C_{55}^{\{1\}}\left[H_1D_1\sum_{j=2}^{K-1}A_{Xkj}^{[1]}\overline{W}^{(1)}(X_j,Y_m,0)+\frac{1}{D_1}\sum_{f=1}^{R_1}A_{Z1f}^{[1]}\overline{U}^{(1)}(X_k,Y_m,Z_f)\right]=0$$

$$C_{44}^{\{1\}}\left[H_1\frac{D_1}{B_\mathrm{p}}\sum_{g=2}^{M-1}A_{Ymg}^{[1]}\overline{W}^{(1)}(X_k,Y_g,0)+\frac{B_\mathrm{p}}{D_1}\sum_{f=1}^{R_1}A_{Z1f}^{[1]}\overline{V}^{(1)}(X_k,Y_m,Z_f)\right]=0$$

at the bottom surface of the bottom layer and

$$C_{31}^{\{L\}}\sum_{j=1}^{K}A_{Xkj}^{[1]}\overline{U}^{(L)}(X_j,Y_m,H)+C_{32}^{\{L\}}\sum_{g=1}^{M}A_{Ymg}^{[1]}\overline{V}^{(L)}(X_k,Y_g,H)+C_{33}^{\{L\}}H_L\sum_{f=1}^{R_L}A_{ZR_Lf}^{[1]}\overline{W}^{(L)}(X_k,Y_m,Z_f)=-q(X_k,Y_m)$$

$$C_{55}^{\{L\}}\left[H_LD_L\sum_{j=2}^{K-1}A_{Xkj}^{[1]}\overline{W}^{(L)}(X_j,Y_m,H)+\frac{1}{D_L}\sum_{f=1}^{R_L}A_{ZR_Lf}^{[1]}\overline{U}^{(L)}(X_k,Y_m,Z_f)\right]=0$$

$$C_{44}^{\{L\}}\left[H_L\frac{D_L}{B_\mathrm{p}}\sum_{g=2}^{M-1}A_{Ymg}^{[1]}\overline{W}^{(L)}(X_k,Y_g,H)+\frac{B_\mathrm{p}}{D_L}\sum_{f=1}^{R_L}A_{ZR_Lf}^{[1]}\overline{V}^{(L)}(X_k,Y_m,Z_f)\right]=0$$

at the top surface of the top layer

(25)

The normalised DQ interlaminar continuity conditions at an interior grid point $(X_k,Y_m,H_i^{\mathrm{T}})$ can be expressed as

$$\begin{aligned}
&C_{31}^{\{i\}}\sum_{j=1}^{K}A_{Xkj}^{[1]}\overline{U}^{(i)}(X_j,Y_m,H_i^{\mathrm{T}})+C_{32}^{\{i\}}\sum_{g=1}^{M}A_{Ymg}^{[1]}\overline{V}^{(i)}(X_k,Y_g,H_i^{\mathrm{T}})+C_{33}^{\{i\}}H_i\sum_{f=1}^{R_i}A_{ZR_if}^{[1]}\overline{W}^{(i)}(X_k,Y_m,Z_f)\\
&\quad=\frac{E}{(1+\nu)\cdot(1-2\nu)}\left\{(1-\nu)\cdot(\overline{W}^{(i)}-\overline{W}^{(i+1)})\frac{H}{h}\right.\\
&\qquad\left.+\nu\cdot\left[\sum_{j=1}^{K}A_{Xkj}^{[1]}\overline{U}^{(i)}(X_j,Y_m,H_i^{\mathrm{T}})+\sum_{g=1}^{M}A_{Ymg}^{[1]}\overline{V}^{(i)}(X_k,Y_g,H_i^{\mathrm{T}})\right]\right\}\\
&C_{55}^{\{i\}}\left[H_iD_i\sum_{j=2}^{K-1}A_{Xkj}^{[1]}\overline{W}^{(i)}(X_j,Y_m,H_i^{\mathrm{T}})+\frac{1}{D_i}\sum_{f=1}^{R_i}A_{ZR_if}^{[1]}\overline{U}^{(i)}(X_k,Y_m,Z_f)\right]\\
&\quad=G\cdot\left[H_iD_i\sum_{j=2}^{K-1}A_{Xkj}^{[1]}\overline{W}^{(i)}(X_j,Y_m,H_i^{\mathrm{T}})+\frac{a}{h}\left(\overline{U}^{(i)}-\overline{U}^{(i+1)}\right)\right]\\
&C_{44}^{\{i\}}\left[H_i\frac{D_i}{B_\mathrm{p}}\sum_{g=2}^{M-1}A_{Ymg}^{[1]}\overline{W}^{(i)}(X_k,Y_g,H_i^{\mathrm{T}})+\frac{B_\mathrm{p}}{D_i}\sum_{f=1}^{R_i}A_{ZR_if}^{[1]}\overline{V}^{(i)}(X_k,Y_m,Z_f)\right]\\
&\quad=G\cdot\left[H_i\frac{D_i}{B_\mathrm{p}}\sum_{g=2}^{M-1}A_{Ymg}^{[1]}\overline{W}^{(i)}(X_k,Y_g,H_i^{\mathrm{T}})+\frac{b}{h}\left(\overline{V}^{(i)}-\overline{V}^{(i+1)}\right)\right]
\end{aligned}\tag{26}$$

where $H_i^{\mathrm{T}}$ denotes the thickness coordinate at interface between lower lamina and bonding layer, and correspondingly at $(X_k,Y_m,H_{i+1}^{B})$

$$
\begin{aligned}
&\frac{E}{(1+v)\cdot(1-2v)}\left\{(1-v)\cdot\left(\overline{W}^{(i)}-\overline{W}^{(i+1)}\right)\frac{H}{h}\right.\\
&\qquad\left.+\,v\left[\sum_{j=1}^{K}A^{[1]}_{Xkj}\overline{U}^{(i+1)}(X_j,Y_m,H^B_{i+1})+\sum_{g=1}^{M}A^{[1]}_{Ymg}\overline{V}^{(i+1)}(X_k,Y_g,H^B_{i+1})\right]\right\}\\
&\quad=C^{\{i+1\}}_{31}\sum_{j=1}^{K}A^{[1]}_{Xkj}\overline{U}^{(i+1)}(X_j,Y_m,H^B_{i+1})\\
&+C^{\{i+1\}}_{32}\sum_{g=1}^{M}A^{[1]}_{Ymg}\overline{V}^{(i+1)}(X_k,Y_g,H^B_{i+1})+C^{\{i+1\}}_{33}H_{i+1}\sum_{f=1}^{R_{i+1}}A^{[1]}_{Z1f}\overline{W}^{(i+1)}\left(X_k,Y_m,Z_f\right)\\
&G\cdot\left[H_{i+1}D_{i+1}\sum_{j=2}^{K-1}A^{[1]}_{Xkj}\overline{W}^{(i+1)}(X_j,Y_m,H^B_{i+1})+\frac{a}{h}(\overline{U}^{(i)}-\overline{U}^{(i+1)})\right]\\
&\quad=C^{\{i+1\}}_{55}\left[H_{i+1}D_{i+1}\sum_{j=2}^{K-1}A^{[1]}_{Xkj}\overline{W}^{(i+1)}(X_j,Y_m,H^B_{i+1})+\frac{1}{D_{i+1}}\sum_{f=1}^{R_{i+1}}A^{[1]}_{Z1f}\overline{U}^{(i+1)}(X_k,Y_m,Z_f)\right]\\
&G\cdot\left[H_{i+1}\frac{D_{i+1}}{B_{\mathrm{p}}}\sum_{g=2}^{M-1}A^{[1]}_{Ymg}\overline{W}^{(i+1)}(X_k,Y_g,H^B_{i+1})+\frac{b}{h}(\overline{V}^{(i)}-\overline{V}^{(i+1)})\right]\\
&\quad=C^{\{i+1\}}_{44}\left[H_{i+1}\frac{D_{i+1}}{B_{\mathrm{p}}}\sum_{g=2}^{M-1}A^{[1]}_{Ymg}\overline{W}^{(i+1)}(X_k,Y_g,H^B_{i+1})+\frac{B_{\mathrm{p}}}{D_{i+1}}\sum_{f=1}^{R_{i+1}}A^{[1]}_{Z1f}\overline{V}^{(i+1)}(X_k,Y_m,Z_f)\right]
\end{aligned}
\tag{27}
$$

where $H^B_{i+1}$ is the thickness coordinate at the interface between the bonding layer and the upper lamina, and $G$ is the shear modulus of the bonding layer.

In this study, various examples of laminates with various edge supports will be provided to demonstrate the advantages of the present methodology. The following abbreviations will be used: SSSS stands for simple support at the four edges, and SCSC for simple support at the two opposing edges and clamped support at the other two edges. Finally, CCCC refers to clamp support at the four edges. For the following analyses, $E$, $h$ and $v$ denote the modulus, thickness and Poisson's ratio of the bonding layers.

## 3. Results and discussions

In this first example, we examine a three-ply (0°/90°/0°) simply supported square sandwich laminates of various moduli ratios under uniform surface pressure. The material properties of the surface layers were the same as those used by Srinivas and Rao (1970)

$$
\begin{aligned}
&\frac{E_y}{E_x}=0.543103,\quad \frac{E_z}{E_x}=0.530172,\quad \frac{E_{xy}}{E_x}=0.23319,\quad \frac{E_{xz}}{E_x}=0.010776\\
&\frac{E_{yz}}{E_x}=0.098276,\quad \frac{G_{xy}}{E_x}=0.262931,\quad \frac{G_{xz}}{E_x}=0.159914,\quad \frac{G_{yz}}{E_x}=0.26681
\end{aligned}
\tag{28}
$$

Variations of the ratios of material properties of the core layer to the surface layers are subsequently considered. The thickness of the top and bottom plies is assumed to be one-tenth the thickness of the laminates, while the latter is one-tenth of the in-plane dimension of the laminates. The transverse mesh employed in this example is three grid points within the top and bottom plies, and five grid points in the core layer, while the in-plane mesh grid distributions are listed in Table 1. The table shows a comparison

Table 1
Comparison of normalised central deflections ($WE_{x2}/Hq$) of simply supported square sandwich laminates [0°/90°/0°]

| $E_{x1}/E_{x2}$ | $E/E_{x2}$ | $h$ (in.) | $v$ | $7 \times 7$ | $9 \times 9$ | $11 \times 11$ | $13 \times 13$ |
|---|---|---|---|---|---|---|---|
| 1 | 0.01 | $10^{-3}$ | 0.01 | 757.68 | 754.79 | 751.55 | 751.27 |
| | | | 0.3 | 758.40 | 755.57 | 752.36 | 752.09 |
| | | $10^{-5}$ | 0.01 | – | – | – | – |
| | | | 0.3 | 758.40 | 755.32 | 751.99 | 751.65 |
| | | $10^{-7}$ | 0.01 | 759.13 | 756.03 | 752.70 | 752.36 |
| | | | 0.3 | 759.13 | 756.03 | 752.70 | 752.36 |
| | 0.1 | $10^{-3}$ | 0.01 | – | – | – | – |
| | | | 0.3 | 749.26 | 746.35 | 743.11 | 742.79 |
| | | $10^{-5}$ | 0.01 | – | – | – | – |
| | | | 0.3 | 758.31 | 755.22 | 751.90 | 751.56 |
| | | $10^{-7}$ | 0.01 | – | – | – | – |
| | | | 0.3 | 759.13 | 756.03 | 752.70 | 752.36 |
| | 1 | $10^{-3}$ | 0.01 | 754.96 | 751.90 | 748.60 | 748.26 |
| | | | 0.3 | 679.77 | 677.97 | 675.24 | 674.98 |
| | | $10^{-5}$ | 0.01 | – | – | – | – |
| | | | 0.3 | 757.53 | 754.46 | 751.14 | 750.80 |
| | | $10^{-7}$ | 0.01 | 759.13 | 756.03 | 752.70 | 752.36 |
| | | | 0.3 | 759.12 | 756.02 | 752.69 | 752.35 |
| | 10 | $10^{-3}$ | 0.01 | 741.54 | 738.72 | 735.52 | 735.19 |
| | | | 0.3 | 351.01 | 352.17 | 351.33 | 351.27 |
| | | $10^{-5}$ | 0.01 | – | – | – | – |
| | | | 0.3 | 749.82 | 746.88 | 743.62 | 743.29 |
| | | $10^{-7}$ | 0.01 | 759.12 | 756.02 | 752.68 | 752.32 |
| | | | 0.3 | 759.03 | 755.97 | 752.60 | 752.25 |
| Srinivas and Rao (1970) | | | | 688.58 | | | |
| {DQR} | | | | 690.96 | | | |
| 5 | 0.01 | $10^{-3}$ | 0.01 | 290.72 | 292.07 | 291.59 | 291.67 |
| | | | 0.3 | 291.06 | 292.43 | 291.95 | 292.04 |
| | | $10^{-5}$ | 0.01 | – | – | – | – |
| | | | 0.3 | 290.91 | 292.21 | 291.73 | 291.80 |
| | | $10^{-7}$ | 0.01 | 291.45 | 292.75 | 292.26 | 292.34 |
| | | | 0.3 | 291.45 | 292.75 | 292.26 | 292.34 |
| | 0.1 | $10^{-3}$ | 0.01 | – | – | – | – |
| | | | 0.3 | 284.65 | 285.96 | 285.49 | 285.57 |
| | | $10^{-5}$ | 0.01 | – | – | – | – |
| | | | 0.3 | 290.84 | 292.15 | 291.66 | 291.73 |
| | | $10^{-7}$ | 0.01 | – | – | – | – |
| | | | 0.3 | 291.45 | 292.75 | 292.26 | 292.34 |
| | 1 | $10^{-3}$ | 0.01 | 288.96 | 290.27 | 289.28 | 289.97 |
| | | | 0.3 | 238.01 | 239.32 | 238.94 | 239.01 |
| | | $10^{-5}$ | 0.01 | – | – | – | – |
| | | | 0.3 | 290.26 | 291.57 | 291.08 | 291.16 |
| | | $10^{-7}$ | 0.01 | 291.45 | 292.75 | 292.26 | 292.34 |
| | | | 0.3 | 291.44 | 292.75 | 292.26 | 292.33 |
| | 10 | $10^{-3}$ | 0.01 | 279.23 | 280.53 | 280.07 | 280.15 |
| | | | 0.3 | 89.40 | 90.07 | 89.97 | 90.00 |
| | | $10^{-5}$ | 0.01 | – | – | – | – |
| | | | 0.3 | 284.61 | 285.92 | 285.45 | 285.52 |
| | | $10^{-7}$ | 0.01 | 291.45 | 292.76 | 292.27 | 292.30 |

(*continued on next page*)

Table 1 (*continued*)

| $E_{x1}/E_{x2}$ | $E/E_{x2}$ | $h$ (in.) | $v$ | $7 \times 7$ | $9 \times 9$ | $11 \times 11$ | $13 \times 13$ |
|---|---|---|---|---|---|---|---|
| | | | 0.3 | 291.39 | 292.66 | 292.16 | 292.24 |
| Srinivas and Rao (1970) | | | | 258.97 | | | |
| {DQR} | | | | 260.38 | | | |

$E_{x1}$ is elastic modulus of the surface layers and $E_{x2}$ is elastic modulus of the core layer.

between the numerical results of central deflections obtained from the current 3D model of elastic bonding with the analytical solutions of Srinivas and Rao (1970) based on a rigid bonding model. "DQR" refers to results of rigid bonding model using the present DQ methodology. It can be observed that the present model exhibits stable convergence characteristics. The results shown in Table 1 are quite distinct from those of Srinivas and Rao (1970), stemming from the weakened rigidity of the elastically bonded sandwich structures when compared with rigidly bonded structures treated by Srinivas and Rao (1970). The results also reveal that the present approach is capable of accurately accounting for the influence of the parameters which define the bonding layer; namely, the thickness, elastic modulus and Poisson's ratio. This is due to the fact that the current DQ model employs rigorous three-dimensional elastic modelling techniques.

Table 2 gives the distribution of the normal stress $\sigma_x$ through the thickness. The softer elastic bonding results in the top ply carrying slightly larger stresses. As such, the central deflection and the stress $\sigma_x$ are generally larger when compared with the corresponding results of the rigid bonding case of Srinivas and Rao (1970).

Table 2
Comparison of normalised central normal stress ($\sigma_x/q$) of simply supported square sandwich laminates [0°/90°/0°] for $v = 0.3$

| $E_{x1}/E_x$ | $h$ (in.) | $E/E_{x2}$ | Bottom ply at bottom surface | Bottom ply at interface | Mid ply at lower interface | Mid ply at upper interface | Top ply at interface | Top ply at top surface |
|---|---|---|---|---|---|---|---|---|
| 1 | $10^{-3}$ | 0.01 | 38.350 | 30.256 | 30.282 | −31.507 | −31.469 | −39.631 |
| | | 0.1 | 37.966 | 29.982 | 29.911 | −31.097 | −31.167 | −39.233 |
| | | 1 | 34.354 | 27.124 | 27.050 | −28.140 | −28.214 | −35.479 |
| | $10^{-5}$ | 0.01 | 38.707 | 30.618 | 30.618 | −31.032 | −31.031 | −39.153 |
| | | 0.1 | 38.817 | 30.748 | 30.747 | −30.895 | −30.896 | −39.035 |
| | | 1 | 38.500 | 30.450 | 30.449 | −31.062 | −31.063 | −39.074 |
| Srinivas and Rao (1970) | | | 35.937 | 28.454 | 28.454 | −28.538 | −28.538 | −36.021 |
| {DQR} | | | 36.053 | 28.544 | 28.544 | −28.599 | −28.599 | −36.109 |
| 5 | $10^{-3}$ | 0.01 | 67.242 | 52.146 | 10.427 | −10.598 | −52.932 | −67.856 |
| | | 0.1 | 65.851 | 51.096 | 10.191 | −10.365 | −51.888 | −66.472 |
| | | 1 | 54.696 | 42.497 | 8.4719 | −8.6360 | −43.242 | −55.272 |
| | $10^{-5}$ | 0.01 | 67.058 | 51.759 | 10.351 | −10.583 | −52.836 | −68.297 |
| | | 0.1 | 66.943 | 51.865 | 10.372 | −10.607 | −52.963 | −67.846 |
| | | 1 | 67.314 | 52.043 | 10.408 | −10.479 | −52.317 | −67.735 |
| Srinivas and Rao (1970) | | | 60.155 | 46.426 | 9.2845 | −9.3402 | −46.623 | −60.353 |
| {DQR} | | | 60.412 | 46.621 | 9.323 | −9.368 | −46.760 | −60.558 |

$E_{x1}$ is elastic modulus of the surface layers and $E_{x2}$ is elastic modulus of the core layer.

Table 3
Comparison of normalised central deflections, $W \times 10^6/q$, (panel A) and central stresses $\sigma_x/q$ (panel B) of simply supported laminates [0°/90°/0°] for $a = 200$ in

| $a/b$ | $h$ (in.) | | $E = 10^6$ | | $E = 15 \times 10^6$ | | $E = 20 \times 10^6$ | |
|---|---|---|---|---|---|---|---|---|
| | | | $v = 0.01$ | $v = 0.3$ | $v = 0.01$ | $v = 0.3$ | $v = 0.01$ | $v = 0.3$ |
| *Panel A* | | | | | | | | |
| $H/a = 0.14$ | | | | | | | | |
| 3 | $10^{-3}$ | Present | 15.199 | 15.194 | 15.198 | 15.190 | 15.198 | 15.186 |
| | | ANSYS | 14.886 | 14.886 | 14.885 | 14.885 | 14.885 | 14.885 |
| | $10^{-7}$ | Present | 15.201 | 15.199 | 15.201 | 15.198 | 15.201 | 15.197 |
| | | ANSYS | 14.888 | 14.888 | 14.888 | 14.888 | 14.888 | 14.888 |
| Liew et al. (1996) {DQR} | | | | | 14.399<br>14.432 | | | |
| 5 | $10^{-3}$ | Present | 2.9893 | 2.9892 | 2.9892 | 2.9888 | 2.9892 | 2.9884 |
| | | ANSYS | 3.0203 | 3.0203 | 3.0201 | 3.0201 | 3.0201 | 3.0201 |
| | $10^{-7}$ | Present | 2.9896 | 2.9896 | 2.9896 | 2.9895 | 2.9896 | 2.9895 |
| | | ANSYS | 3.0206 | 3.0206 | 3.0206 | 3.0206 | 3.0206 | 3.0206 |
| Liew et al. (1996) {DQR} | | | | | 3.0326<br>2.9568 | | | |
| $H/a = 0.2$ | | | | | | | | |
| 3 | $10^{-3}$ | Present | 6.7138 | 6.7135 | 6.7137 | 6.7128 | 6.7137 | 6.7122 |
| | | ANSYS | 6.7334 | 6.7334 | 6.7331 | 6.7332 | 6.7330 | 6.7331 |
| | $10^{-7}$ | Present | 6.7145 | 6.7144 | 6.7145 | 6.7144 | 6.7145 | 6.7143 |
| | | ANSYS | 6.7339 | 6.7339 | 6.7339 | 6.7339 | 6.7339 | 6.7339 |
| Liew et al. (1996) {DQR} | | | | | 6.5260<br>6.4197 | | | |
| 5 | $10^{-3}$ | Present | 1.4334 | 1.4335 | 1.4334 | 1.4334 | 1.4334 | 1.4334 |
| | | ANSYS | 1.6096 | 1.6096 | 1.6095 | 1.6095 | 1.6095 | 1.6095 |
| | $10^{-7}$ | Present | 1.4335 | 1.4336 | 1.4335 | 1.4336 | 1.4335 | 1.4336 |
| | | ANSYS | 1.6097 | 1.6097 | 1.6097 | 1.6097 | 1.6097 | 1.6097 |
| Liew et al. (1996) {DQR} | | | | | 1.6113<br>1.4245 | | | |
| *Panel B* | | | | | | | | |
| $H/a = 0.14$ | | | | | | | | |
| 3 | $10^{-3}$ | Present | 2.3987 | 2.3926 | 2.3986 | 2.3892 | 2.3986 | 2.3856 |
| | | ANSYS | 2.0670 | 2.0670 | 2.0670 | 2.0670 | 2.0669 | 2.0669 |
| | $10^{-7}$ | Present | 2.2398 | 2.3001 | 2.3508 | 2.2272 | 2.4304 | 2.2479 |
| | | ANSYS | 2.0672 | 2.0672 | 2.0672 | 2.0672 | 2.0672 | 2.0672 |
| Liew et al. (1996) {DQR} | | | | | 1.9580<br>2.0997 | | | |
| 5 | $10^{-3}$ | Present | 0.9947 | 0.9949 | 0.9947 | 0.9949 | 0.9947 | 0.9950 |
| | | ANSYS | 0.6695 | 0.6695 | 0.6695 | 0.6695 | 0.6695 | 0.6695 |
| | $10^{-7}$ | Present | 0.9973 | 0.9936 | 0.9967 | 0.9976 | 0.9923 | 0.9979 |
| | | ANSYS | 0.6696 | 0.6696 | 0.6696 | 0.6696 | 0.6696 | 0.6696 |
| Liew et al. (1996) {DQR} | | | | | 0.6549<br>0.7192 | | | |
| $H/a = 0.2$ | | | | | | | | |
| 3 | $10^{-3}$ | Present | 1.4299 | 1.4291 | 1.4309 | 1.4308 | 1.4304 | 1.4300 |
| | | ANSYS | 1.0416 | 1.0416 | 1.0415 | 1.0415 | 1.0415 | 1.0415 |

(*continued on next page*)

Table 3 (*continued*)

| $a/b$ | $h$ (in.) | | $E = 10^6$ | | $E = 15 \times 10^6$ | | $E = 20 \times 10^6$ | |
|---|---|---|---|---|---|---|---|---|
| | | | $v = 0.01$ | $v = 0.3$ | $v = 0.01$ | $v = 0.3$ | $v = 0.01$ | $v = 0.3$ |
| | $10^{-7}$ | Present | 1.4376 | 1.4158 | 1.4353 | 1.4487 | 1.4345 | 1.4170 |
| | | ANSYS | 1.0416 | 1.0416 | 1.0416 | 1.0416 | 1.0416 | 1.0416 |
| Liew et al. (1996) {DQR} | | | | | 0.9350<br>1.0421 | | | |
| 5 | $10^{-3}$ | Present | 0.5485 | 0.5542 | 0.5497 | 0.5397 | 0.5343 | 0.5393 |
| | | ANSYS | 0.3416 | 0.3416 | 0.3416 | 0.3416 | 0.3416 | 0.3416 |
| | $10^{-7}$ | Present | 0.5997 | 0.5718 | 0.5635 | 0.5765 | 0.5737 | 0.5806 |
| | | ANSYS | 0.3416 | 0.3416 | 0.3416 | 0.3416 | 0.3416 | 0.3416 |
| Liew et al. (1996) {DQR} | | | | | 0.3192<br>0.3216 | | | |

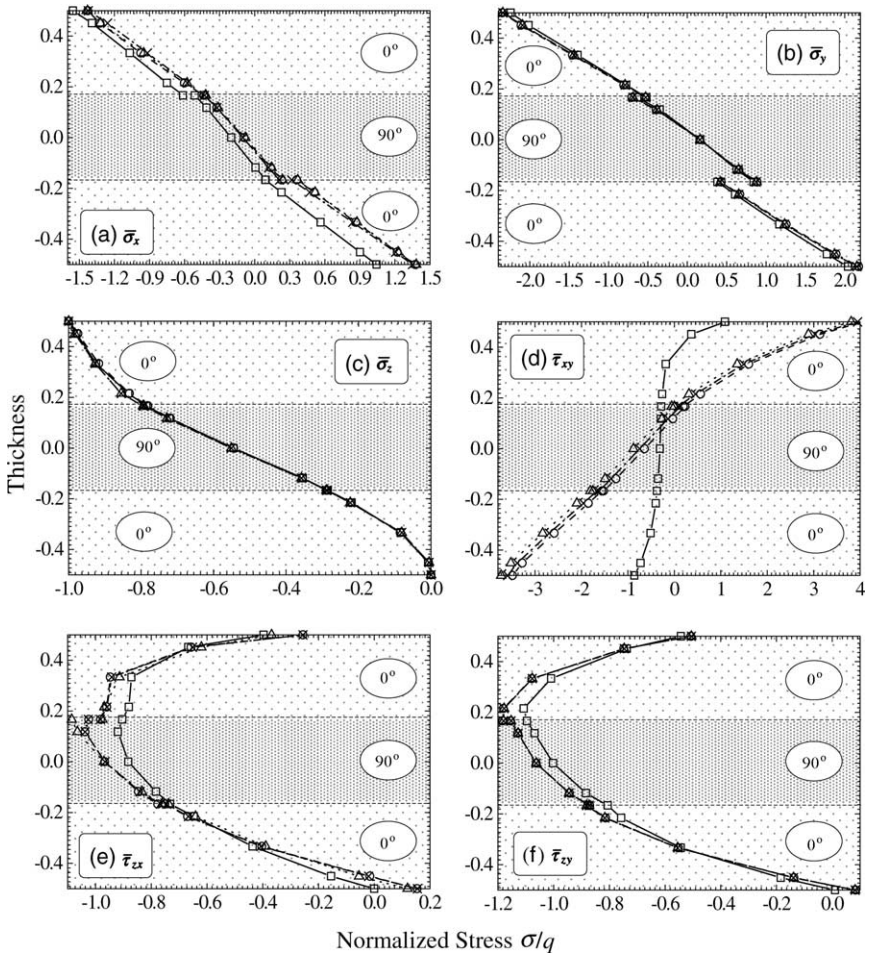


Fig. 2. Stress distributions through thickness of three-ply (0°/90°/0°) laminates ($H/a = 0.2$, $a/b = 3$, $h = 10^{-3}$, $v = 0.3$ and $a = 200$ in.) with SSSS edge conditions, under uniform load. (—□—, rigid bonding; ----○----, $E = 10^6$; ···×···, $E = 15 \times 10^6$; ··· △ ···, $E = 20 \times 10^6$).

The second example considers the global response of three-ply (identical thickness) (0°/90°/0°) simply supported rectangular laminates of various in-plane dimensions under uniform surface pressure. The material properties are similar to those used by Liew et al. (1996)

$$\begin{aligned} &\frac{E_1}{E_0} = 20.83, \quad \frac{E_2}{E_0} = 10.94, \quad \frac{E_3}{E_2} = 1 \\ &\frac{G_{12}}{E_0} = 6.10, \quad \frac{G_{13}}{E_0} = 3.71, \quad \frac{G_{23}}{E_0} = 6.19 \\ &v_{12} = v_{13} = v_{23} = 0.44 \end{aligned} \tag{29}$$

The results which are summarised in Table 3 reveal that the present elastic bonding model is quite distinct from the earlier rigid and weak bonding models. This is because the introduction of the elastic

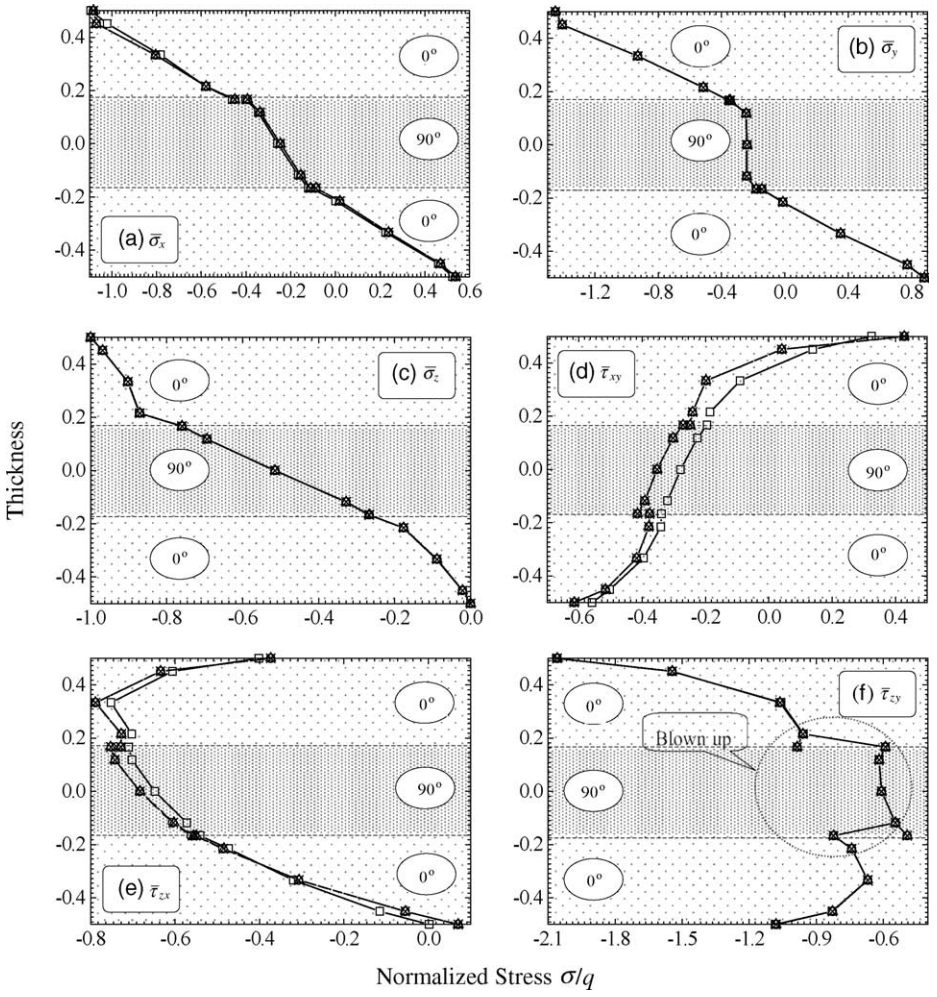


Fig. 3. Stress distributions through thickness of three-ply (0°/90°/0°) laminates ($H/a = 0.2$, $a/b = 3$, $h = 10^{-3}$, $v = 0.3$ and $a = 200$ in.) with SCSC edge conditions, under uniform load. (—□—, rigid bonding; ----○----, $E = 10^6$; ···×···, $E = 15 \times 10^6$; ··· △ ···, $E = 20 \times 10^6$).

bonding layer influences the structural rigidity of the laminate. Interestingly, when the in-plane dimension ratio of the laminate is quite large, i.e. the plate becomes beam-like, the central deflection approaches that of the rigid bonding assumption.

For verification purposes, FE analysis was conducted using the commercial code ANSYS version 6.0. Eight-noded quadrilateral element SHELL99 was used to model this problem. The SHELL99 element may be used for layered shell structures, allowing for up to 250 layers. This element has six degrees-of-freedom at each node, namely translations in the nodal $x$, $y$, $z$ directions and rotations about the nodal $x$, $y$, $z$ axes. Converged results are obtained using a mesh distribution of $10 \times 6$ elements for the case $a/b = 3$, and $20 \times 6$ element for the case $a/b = 5$. Table 3 indicates that the results obtained are in general comparable to those obtained from the present model. The slight discrepancies are due to the fact that SHELL99 cannot accommodate transverse deformation and stresses, thus limiting its accuracy.

Let us now consider the influence of the mechanical properties of the bonding layer upon the central deflection. For the case where $a/b = 3$ and $H/a = 0.14$, the rigid bonding model yields a normalised central deflection $W = 14.432$, which is normalised by $10^6/q$, with $q$ being the surface pressure. In the present

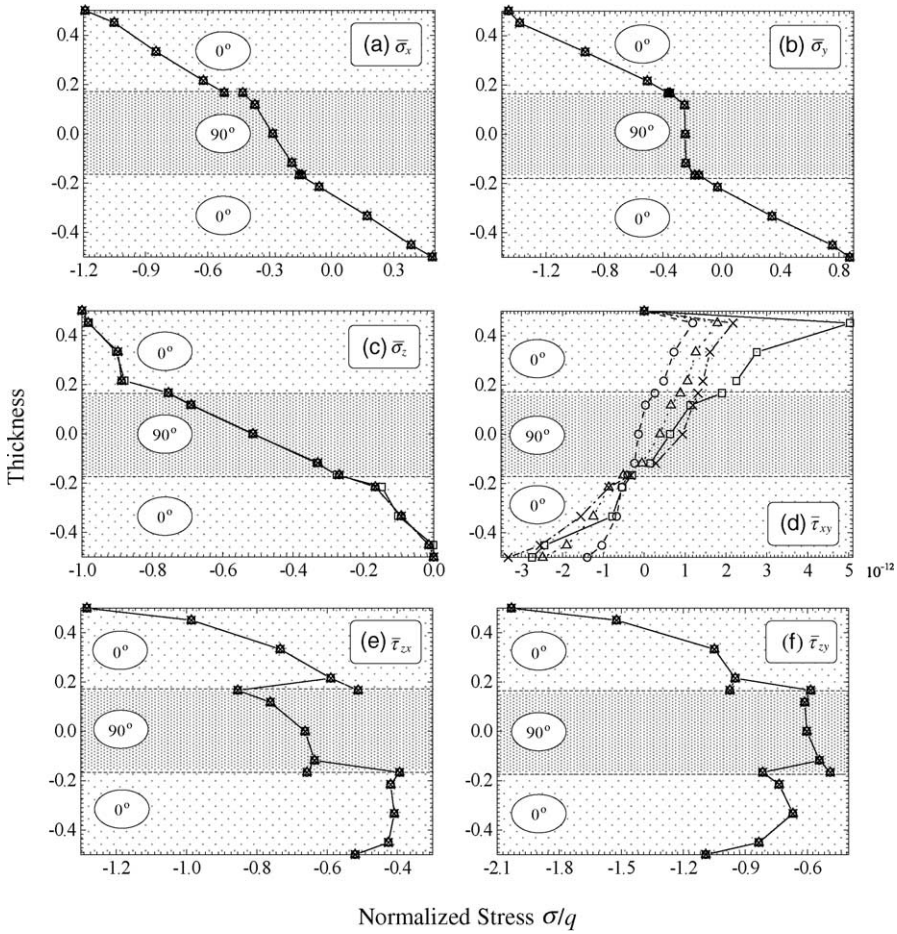


Fig. 4. Stress distributions through thickness of three-ply (0°/90°/0° ) laminates ($H/a = 0.2$, $a/b = 3$, $h = 10^{-3}$, $v = 0.3$ and $a = 200$ in.) with CCCC edge conditions, under uniform load. (—□—, rigid bonding; ----○----, $E = 10^6$; ···×···, $E = 15 \times 10^6$; ···△··· $E = 20 \times 10^6$).

elastic bonding model ($v = 0.3$ and $h = 10^{-3}$ in.), for $E = 10^8$, $W = 15.144$; for $E = 5 \times 10^8$, $W = 14.914$; and when $E = 10^9$, $W = 14.6385$. This shows that when the bonding layer stiffens, the global deflection of the structure approaches that of the rigid bonding model.

Figs. 2–4 show the variation of the normal and shear stresses through the thickness of the laminate. The results also reveal that the maximum normal stresses occur at the centre of the plate while the maximum shear stresses $\tau_{xy}$, $\tau_{xz}$ and $\tau_{yz}$ occur at locations $(0, 0)$, $(0, b/2)$, and $(a/2, 0)$, respectively. One exceptional case is the distribution of $\tau_{xy}$ for the fully clamped case where the maximum is located at the central point. Fig. 2 contrasts the stress distributions through thickness in laminated composites modelled in terms of the rigid and elastic bonding assumptions. It reveals that both sets of results are distinctly different, especially for the shear stress distribution.

In the third example, we consider three-ply laminates (0°/90°/0°) with identical thickness and different support, with the same material properties as those of the last example. The elastic bonding model reveals that significant discrepancies exist between the above shear stresses and those calculated using the rigid bonding model. Table 4 and Fig. 3, and Table 5 and Fig. 4, illustrate the various central deflections and stress distributions for laminates under support conditions of mixed clamped and fully clamped types, respectively. We will now examine the transverse shear stress distributions for the various support configurations in Figs. 2–4. The results show that for the simply supported SSSS and simply supported-clamped SCSC cases, even with the present elastic bonding model, there is only a limited difference between the transverse shear stresses of adjoining plies. However, in the fully clamped CCCC case, the usefulness of

Table 4
Comparison of normalised central deflections ($W \times 10^6/q$) of SCSC-supported laminates [0°/90°/0°], where the simply-supported edges are at $x = 0$ and $a$, and clamped edges are at $y = 0$ and $b$ for the case $a = 200$ in.

| $a/b$ | $h$ (in.) | $E = 10^6$ | | | $E = 15 \times 10^6$ | | | $E = 20 \times 10^6$ | | |
|---|---|---|---|---|---|---|---|---|---|---|
| | | $v = 0.2$ | $v = 0.3$ | $v = 0.4$ | $v = 0.2$ | $v = 0.3$ | $v = 0.4$ | $v = 0.2$ | $v = 0.3$ | $v = 0.4$ |
| $H/a = 0.14$ | | | | | | | | | | |
| | $10^{-3}$ | 6.9836 | 6.9835 | 6.9831 | 6.9831 | 6.9826 | 6.9812 | 6.9827 | 6.9818 | 6.9794 |
| 3 | $10^{-5}$ | 6.9844 | 6.9843 | 6.9839 | 6.9844 | 6.9842 | 6.9836 | 6.9843 | 6.9840 | 6.9833 |
| | $10^{-7}$ | 6.9844 | 6.9842 | 6.9839 | 6.9843 | 6.9841 | 6.9835 | 6.9843 | 6.9840 | 6.9832 |
| Liew et al. (1996) {DQR} | | | | | | 6.7577<br>6.9784 | | | | |
| | $10^{-3}$ | 1.8397 | 1.8397 | 1.8398 | 1.8396 | 1.8395 | 1.8394 | 1.8395 | 1.8394 | 1.8391 |
| 5 | $10^{-5}$ | 1.8398 | 1.8398 | 1.8398 | 1.8398 | 1.8398 | 1.8397 | 1.8398 | 1.8397 | 1.8397 |
| | $10^{-7}$ | 1.8398 | 1.8398 | 1.8398 | 1.8398 | 1.8398 | 1.8397 | 1.8398 | 1.8398 | 1.8397 |
| Liew et al. (1996) {DQR} | | | | | | 1.8913<br>1.8386 | | | | |
| $H/a = 0.2$ | | | | | | | | | | |
| | $10^{-3}$ | 3.9047 | 3.9047 | 3.9048 | 3.9046 | 3.9045 | 3.9042 | 3.9044 | 3.9042 | 3.9036 |
| 3 | $10^{-5}$ | 3.9050 | 3.9049 | 3.9048 | 3.9050 | 3.9049 | 3.9048 | 3.9049 | 3.9049 | 3.9047 |
| | $10^{-7}$ | 3.9050 | 3.9049 | 3.9049 | 3.9050 | 3.9049 | 3.9048 | 3.9050 | 3.9049 | 3.9047 |
| Liew et al. (1996) {DQR} | | | | | | 3.9116<br>3.9020 | | | | |
| | $10^{-3}$ | 1.0760 | 1.0760 | 1.0761 | 1.0760 | 1.0760 | 1.760 | 1.0759 | 1.0759 | 1.0759 |
| 5 | $10^{-5}$ | 1.0761 | 1.0761 | 1.0761 | 1.0761 | 1.0761 | 1.0761 | 1.0761 | 1.0761 | 1.0761 |
| | $10^{-7}$ | 1.0761 | 1.0761 | 1.0761 | 1.0761 | 1.0761 | 1.0761 | 1.0761 | 1.0761 | 1.0761 |
| Liew et al. (1996) {DQR} | | | | | | 1.2202<br>1.0757 | | | | |

Table 5
Comparison of normalised central deflections ($W \times 10^6/q$) of fully clamped (CCCC) laminates [0°/90°/0°] $a = 200$ in.

| $a/b$ | $h$ (in.) | $E = 10^6$ | | | $E = 15 \times 10^6$ | | | $E = 20 \times 10^6$ | | |
|---|---|---|---|---|---|---|---|---|---|---|
| | | $v = 0.2$ | $v = 0.3$ | $v = 0.4$ | $v = 0.2$ | $v = 0.3$ | $v = 0.4$ | $v = 0.2$ | $v = 0.3$ | $v = 0.4$ |
| $H/a = 0.14$ | | | | | | | | | | |
| 3 | $10^{-3}$ | 6.9136 | 6.9136 | 6.9136 | 6.9132 | 6.9129 | 6.9121 | 6.9128 | 6.9122 | 6.9106 |
| | $10^{-7}$ | 6.9139 | 6.9138 | 6.9139 | 6.9139 | 6.9139 | 6.9139 | 6.9139 | 6.9139 | 6.9139 |
| Liew et al. (1996) {DQR} | | | | | | 6.6931<br>6.9130 | | | | |
| 5 | $10^{-3}$ | 1.8370 | 1.8371 | 1.8372 | 1.8369 | 1.8369 | 1.8369 | 1.8369 | 1.8368 | 1.8366 |
| | $10^{-7}$ | 1.8370 | 1.8370 | 1.8370 | 1.8370 | 1.8370 | 1.8370 | 1.8370 | 1.8370 | 1.8370 |
| Liew et al. (1996) {DQR} | | | | | | 1.8902<br>1.8368 | | | | |
| $H/a = 0.2$ | | | | | | | | | | |
| 3 | $10^{-3}$ | 3.8655 | 3.8655 | 3.8656 | 3.8653 | 3.8653 | 3.8651 | 3.8652 | 3.8651 | 3.8647 |
| | $10^{-7}$ | 3.8655 | 3.8655 | 3.8655 | 3.8655 | 3.8655 | 3.8655 | 3.8655 | 3.8655 | 3.8655 |
| Liew et al. (1996) {DQR} | | | | | | 3.8696<br>3.8652 | | | | |
| 5 | $10^{-3}$ | 1.0743 | 1.0743 | 1.0744 | 1.0743 | 1.0743 | 1.0743 | 1.0742 | 1.0742 | 1.0742 |
| | $10^{-7}$ | 1.0743 | 1.0743 | 1.0743 | 1.0743 | 1.0743 | 1.0743 | 1.0743 | 1.0743 | 1.0743 |
| Liew et al. (1996) {DQR} | | | | | | 1.2192<br>1.0742 | | | | |

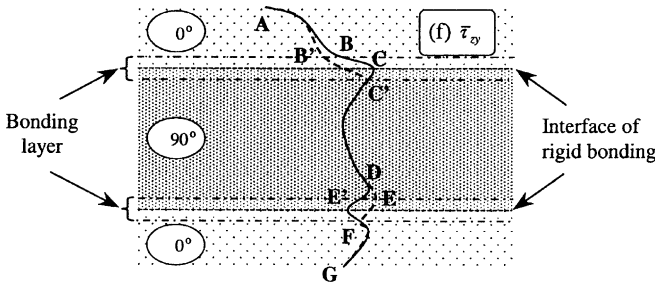


Fig. 5. Blown-up diagram of Fig. 3(f): (- - -) current elastic bonding; (—) rigid bonding.

the present elastic bonding model is clearly evident. In particular, it has enabled us to determine the differences that exist between the transverse shear stresses of adjoining plies. To illustrate this difference more clearly, a blown-up diagram, Fig. 5, is plotted based on Fig. 3(f) as an example. In Fig. 5, the dashed line AB′C′EFG represents the stress distribution obtained through the current elastic bonding model, while the solid line ABCDE′G represents that of the rigid bonding model. The sections B′C′ and EF of elastic bonding cannot be visualized in Figs. 2–4, while points B′, C′, E and F are vertically located along lamina interface for the rigid bonding case.

## 4. Conclusions

Distinct from existing methods, such as the weak and rigid bonding models, this paper presents an elastic bonding model embodied by a material bonding layer. Differential quadrature modelling scheme is de-

veloped, incorporating three-dimensional elasticity theory, in a layerwise framework. Interfacial characteristics of continuity and discontinuity fulfil the kinematic compatibility through the bonding layer. All the physical equations governing the problem are satisfied and the results for some typical cases are investigated. Validation tests through comparisons with finite element analysis and existing results from the open literature are considered. A detailed study of the convergence characteristics of the present formulations has also been conducted. All evidence indicates that the present three-dimensional layerwise DQ model of elastic bonding is robust, effective, and accurate. This can be attributed to the strict theoretical foundation, rational simplification of the bonding model, and the proper exploitation of the DQ method for the computational scheme. Remarkably, the present elastic bonding model establishes a self-adjustable configuration to simulate the diverse bonding characteristics in laminates. Unlike existing rigid or weak bonding models, the present three-dimensional model exposes previously unknown mechanical features in individual lamina.

## Acknowledgements

The authors wish to acknowledge the constructive remarks made by the necessarily anonymous reviewers of the current paper.

## References

Ambartsumyan, S.A., 1970. Theory of anisotropic plates. Technomic, Stanford, CT.

Bellman, R.E., 1973. Methods of Nonlinear Analysis. Academic Press, New York.

Bert, C.W., Malik, M., 1996. Differential quadrature method in computational mechanics: a review. Applied Mechanics Review 49, 1–28.

Bert, C.W., Jang, S.K., Striz, A.G., 1988. Two new approximate methods for analyzing free vibration of structural components. AIAA Journal 26, 612–618.

Farsa, J., Kukreti, A.R., Bert, C.W., 1993. Fundamental frequency analysis of laminated rectangular plates by the differential quadrature method. International Journal for Numerical Methods in Engineering 36, 2341–2356.

Fazio, P., Hussein, R., Ha, K.H., 1982. Beam-columns with interlayer slips. Journal of Engineering Mechanics, ASCE 108, 354–366.

Goodman, J.R., 1967. Layered wood systems with interlayer slip. Ph.D. Dissertation, University of California, Berkeley.

Han, J.B., Liew, K.M., 1997. Numerical differential quadrature method for Reissner/Mindlin plates on two-parameter foundations. International Journal of Mechanical Sciences 39, 977–990.

Jang, S.K., Bert, C.W., Striz, A.G., 1989. Application of differential quadrature to static analysis of structural components. International Journal for Numerical Methods in Engineering 28, 561–577.

Liew, K.M., Han, J.B., Xiao, Z.M., 1996. Differential quadrature method for thick symmetric cross-ply laminates with first-order shear flexibility. International Journal of Solids and Structures 33, 2647–2658.

Liew, K.M., Teo, T.M., Han, J.-B., 1999. Comparative accuracy of DQ and HDQ methods for three-dimensional vibration analysis of rectangular plates. International Journal for Numerical Methods in Engineering 45, 1831–1848.

Liew, K.M., Teo, T.M., Han, J.-B., 2001. Three-dimensional static solutions of rectangular plates by variant differential quadrature method. International Journal of Mechanical Sciences 43, 1611–1628.

Liew, K.M., Ng, T.Y., Zhang, J.Z., 2002. Differential quadrature-layer modeling technique for three-dimensional analysis of cross-ply laminated plates of various edge-supports. Computer Methods in Applied Mechanics and Engineering 191, 3811–3832.

Liu, D., Xu, L., Lu, X., 1994. Stress analysis of imperfect composite laminates with an interlaminar bonding theory. International Journal for Numerical Methods in Engineering 37, 2819–2839.

Lu, X., Liu, D., 1992. Interlayer shear slip theory for cross-ply laminates with nonrigid interfaces. AIAA Journal 30, 1063–1073.

Newmark, N.M., Seiss, C.P., Viest, I.M., 1951. Tests and analysis of composite beams with incomplete interaction. In: Proceedings of the Society for Experimental Stress Analysis, vol. 9(1). Brookfield Center, Brookfield, CT, pp. 73–79.

Rao, K.M., Ghosh, B.G., 1980. Imperfectly bonded unsymmetric laminated beam. Journal of Engineering Mechanics, ASCE 106, 685–697.

Reddy, J.N, 1984a. Energy and variational methods in applied mechanics. John Wiley and Sons, NY.

Reddy, J.N., 1984b. A simple higher-order theory for laminated composite plates. Transactions of ASME Journal of Applied Mechanics 51, 745–752.

Reddy, J.N., 1984c. A refined nonlinear theory of plates with transverse shear deformation. International Journal of Solids and Structures 20, 881–896.

Reddy, J.N., 1987. A generalization of two-dimensional theories of laminated composite plates. Communications in Applied Numerical Methods 3, 173–180.

Reddy, J.N., 1989. On the generalization of displacement-based laminate theories. Applied Mechanics Reviews 42, 213–222.

Shu, C., 1991. Generalized differential-integral quadrature and application to the simulation of incompressible viscous flows including parallel computation. PhD Thesis, University of Glasgow, Scotland.

Srinivas, S., Rao, A.K., 1970. Bending, vibration and buckling of simply supported thick orthotropic rectangular plates and laminates. International Journal of Solids and Structures 6, 1463–1481.

Stavsky, Y., 1965. On the theory of symmetrically heterogeneous plates having the same thickness variation of the elastic moduli. in: Abir, D., Ollendorff F., Reiner, M. (Eds.), Topic in Applied Mechanics. E. Schwerin, Memorial Volume. Elsevier, New York, pp. 105–166.

Toledano, A., Murakami, H., 1988. Shear-deformable two-layer plate theory with interlayer slip. Journal of Engineering Mechanics, ASCE 114, 605–623.

Whitney, J.M., 1987. Structural analysis of laminated anisotropic plates. Technomic, Lancaster, PA.

Whitney, J.M., Leissa, A.W., 1969. Analysis of heterogeneous anisotropic plates. Transactions of ASME Journal of Applied Mechanics 36, 261–266.

Whitney, J.M., Pagano, N.J., 1970. Shear deformation in heterogeneous anisotropic plates. Transactions of ASME Journal of Applied Mechanics 37, 1031–1036.

Yang, P.C., Norris, C.H., Stavsky, Y., 1966. Elastic wave propagation in heterogeneous plates. International Journal of Solids and Structures 2, 665–684.